EUROPEAN SYNCHROTRON RADIATION FACILITY

INSTALLATION EUROPEENNE DE RAYONNEMENT SYNCHROTRON

Experiment Report Form

The double page inside this form is to be filled in by all users or groups of users who have had access to beam time for measurements at the ESRF.

Once completed, the report should be submitted electronically to the User Office via the User Portal:
https://wwws.esrf.fr/misapps/SMISWebClient/protected/welcome.do

Deadlines for submission of Experimental Reports

Experimental reports must be submitted within the period of 3 months after the end of the experiment.

Experiment Report supporting a new proposal ("relevant report")

If you are submitting a proposal for a new project, or to continue a project for which you have previously been allocated beam time, you must submit a report on each of your previous measurement(s):

- even on those carried out close to the proposal submission deadline (it can be a *"preliminary report")*,
- even for experiments whose scientific area is different form the scientific area of the new proposal,
- carried out on CRG beamlines.

You must then register the report(s) as "relevant report(s)" in the new application form for beam time.

Deadlines for submitting a report supporting a new proposal

- 1st March Proposal Round - **5th March**
- 10th September Proposal Round - **13th September**

The Review Committees reserve the right to reject new proposals from groups who have not reported on the use of beam time allocated previously.

Reports on experiments relating to long term projects

Proposers awarded beam time for a long term project are required to submit an interim report at the end of each year, irrespective of the number of shifts of beam time they have used.

Published papers

All users must give proper credit to ESRF staff members and proper mention to ESRF facilities which were essential for the results described in any ensuing publication. Further, they are obliged to send to the Joint ESRF/ ILL library the complete reference and the abstract of all papers appearing in print, and resulting from the use of the ESRF.

Should you wish to make more general comments on the experiment, please note them on the User Evaluation Form, and send both the Report and the Evaluation Form to the User Office.

Instructions for preparing your Report

- fill in a separate form for each project or series of measurements.
- type your report in English.
- include the experiment number to which the report refers.
- make sure that the text, tables and figures fit into the space available.
- if your work is published or is in press, you may prefer to paste in the abstract, and add full reference details. If the abstract is in a language other than English, please include an English translation.

ESRF	**Experiment title:** **Acoustic velocities and crystallography of majorite and Na-majorite**	**Experiment number**: ES-982
Beamline: ID06-LVP	**Date of experiment**: from: 03/06/2021 to: 07/06/2021	**Date of report**: 01/03/2022
Shifts: 12	**Local contact(s)**: Dr W. Crichton & Dr A. Rosenthal	*Received at ESRF:*

Names and affiliations of applicants (* indicates experimentalists):

Dr A R Thomson*, Department of Earth Sciences, University College London

Prof J Brodholt, Department of Earth Sciences, University College London

Miss E Tripoliti, Department of Earth Sciences, University College London

Report:

The travel times of seismic waves through Earth's interior provide one of the few direct constraints on the physical properties of mantle rocks. If carefully compared with experimental and computational measurements of the elastic properties of minerals this data may be interpreted in terms of mantle mineralogy, chemistry and temperature; information that is not otherwise directly attainable. Over several decades our knowledge of Earth's seismic structure has developed from simple 1-D velocity models, constructed from stacked seismograms (Dziewonski and Anderson 1981), into full 3-D tomographic models of Earth's velocity structure (Ritsema et al. 2011). In order to accurately interpret this vast array of high quality data it is absolutely vital there are high quality measurements of the elastic properties of the main Earth forming minerals. At the present time, using currently available mineralogical databases the seismic velocities of the transition zone appear inconsistent with a pyrolytic or piglogitic bulk composition (Irifune et al., 2008), suggesting either that the velocities of the consituent minerals need to be better constrained our our planet's mantle composition differs from the current consensus.

After olivine and its high-pressure polymorphs, garnet is the second most abundant mineral in peridotite and is modally dominant in subducted eclogitic oceanic crust throughout the upper mantle (Holland et al., 2013). Whilst low-pressure garnets (< 6 GPa) almost exclusively follow an $A^{2+}{}_3B^{3+}{}_2Si_3O_{12}$ stoichiometry, at greater depths the number of silicon cations in equilibrium garnets increases beyond 3 due to 2 substitution mechanisms:

$$2B^{3+} = M^{2+} + Si^{4+} \quad (1 - \textit{Mj substitution})$$
$$B^{3+} + M^{2+} = X^{+} + Si^{4+} \quad (2 - \textit{NaMj substitution})$$

Both substitutions are pressure dependent (Akaogi et al., 1977, Dymshits et al., 2013) and result in final products of (1) $MgSiO_3$ majorite or (2) $Na_2MgSi_5O_{12}$ Na-majorite garnet. In natural systems *Mj* and *NaMj* components account for up to ~ 80 mol.% of garnet's chemistry as reflected by the reported suite of ~ 220 majoritic garnets observed as inclusions within sub-lithospheric diamonds. Thus, *Mj* and *NaMj* components can contribute very significantly to the geophysical properties of garnet throughout the Earth's upper mantle. However, there are currently very few

published constraints (experimental and/or computational) on the seismic velocities of these two majoritic garnet endmembers. Thus, it is feasible that the properties of these garnets may explain the discrepancies between observed mantle velocities and those predicted using mineralogical models.

Both of the high-pressure majoritic endmembers (*Mj* and *NaMj*) adopt a tetragonal crystal symmetry when recovered to ambient conditions ($I4_1/a$ or $I4_1/acd$). However, there is published evidence based on microstructural observations of recovered *Mj* samples that $MgSiO_3$ may undergo a second order tetragonal to cubic ($Ia\bar{3}d$) transition at mantle conditions (~ 18 GPa, > 2000 K, Heinemann et al., 1997). There has been no previous study to investigate the *NaMj* endmember in this way. This experiment was the beginning of our project to study the crystallography and seismic velocities of *Mj* and *NaMj* at realistic mantle conditions.

ES-982 was performed in June 2021, via remote access only, due to the travel restrictions associated with COVID-19. Due to these circumstances the four experiments, which were constructed at UCL and shipped to the ESRF had to be loaded and interfaced with the beamline equipment by Dr Crichton, whom we are very grateful to for his assistance. This COVID-19 operation route signifcantly limited the finesse of instrument control, the ability to perform as many experiments as normally expected and the possibility of adapting the experimental protocol in response to observations from previous runs. Despite these difficulties we were successful in obtaining some results as detailed below (table 1).

Table 1: summary of experimental runs performed in es-982

experiment	starting material	Max *PT* conditions	notes
NaMj_1	NaMj garnet (10/4)	16 GPa, ~ 1000 K	• new low background gaskets • good ultrasonic signal before heating • blow-out on initial heating
NaMj_2	NaMj garnet (7/3)	17 GPa, 1600 K	• made *NaPx* on initial heating (pressure loss) • pressurised to make *NaMj* • ultrasonics signal poor • observed cubic – tetragonal transition in *NaMj* on cooling • collected diffraction to 1 bar • ambient *NaMj* structure refined, tetragonal splitting significantly smaller than in Dymshits et al. (2013). More consitent with earlier studies.
Mj_1	enstatite (10/4)	15 GPa, 1400 K	• made clinoenstatite on initial heating (pressure loss) • compressed to try and reach akimotoite + ringwoodite field • the sample geometry changed to be unsuitable for ultrasonics
Mj_2	enstatite (7/3)	18 GPa, 2200 K	• synthesised akimotoite on intial heating • ultrasonics working • majorite-in at ~ 2000 K • annealing to achieve full sample transformation • massive blow-out before data collection could commence

Within the four experimental runs, two suffered catastrophic blow-outs. One (NaMj_1) was due to the failure of the low-background gaskets upon heating. The second (Mj_2) was during sample annealing at > 2000 K. Mj_1 was also a failure as pressure loss upon initial heating for the majorite sample was far greater than expected, such that the conditions of the majorite stability field could not be reached by subsequent compression at high temperature.

The most successful experiment was NaMj_2, during which NaMj was successfully synthesised and crystallogrpahically studied as a function of temperature at ~ 15 GPa, and during room temperature decompression. Data collected upon cooling from ~ 1600K to room temperature revealed a phase transition in *NaMj* indicated by the discontinuous broadening of the peaks width with decreasing temperature (fig 1). This is consistent with a second order phase transition

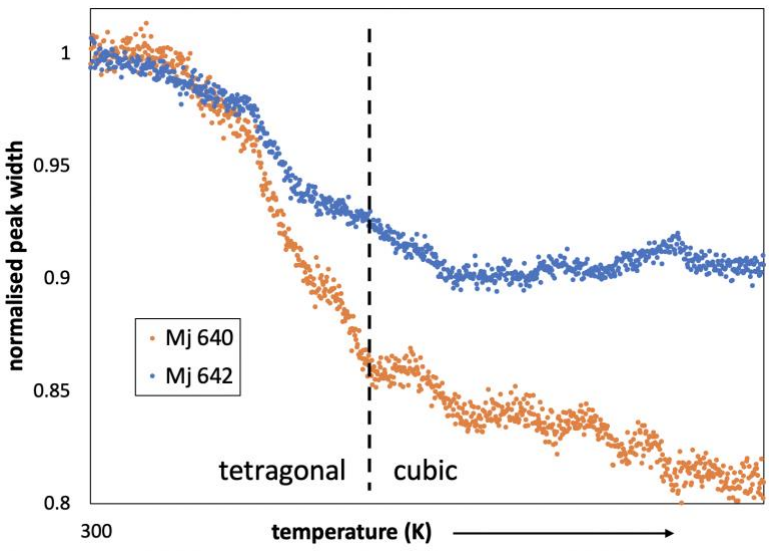

Figure 1: *evolution of the normalised peak width (fwhm relative to 300K) of the 640 and 642 peaks of the NaMj sample as the temperature was reduced from 1600 to 300K. The discontinuity, marked by the deshed vertical line, is consitent with a cubic-tetragonal phase transition.*

from cubic to tetragonal *NaMj*. Unfortunately, the ultraosonic signal, which would have confirmed this observation was poor quality throughout this experiment. After collecting data at a range of high *PT* conditions, diffraction data was collected throughout decompression, revealing the size of tetragonal splitting increases with decreasing pressure towards the ambient sample properties. Full Rietveld refinement of the sample at the end of decompression yields cell parameters for $I4_1/acd$ *NaMj* of a = 11.40764(70) Å, c = 11.40036(71) Å and V = 1483.58(13) $Å^3$ (fig 2). This is an extremely high resolution diffraction pattern, revealing the a/c ratio at ambient conditions of 1.00064(1) and the unit cell volume is constrained to ± 0.009%. These results are quite inconsitent with those of Bindi et al. (2011), but are consitent with earlier reported volumes of Pacalo et al (1992) and Hazen et al (1994). All high PT data is of equally good quality and will provide an extremely good study of the PVT systematics of *NaMj* when combined with additional data.

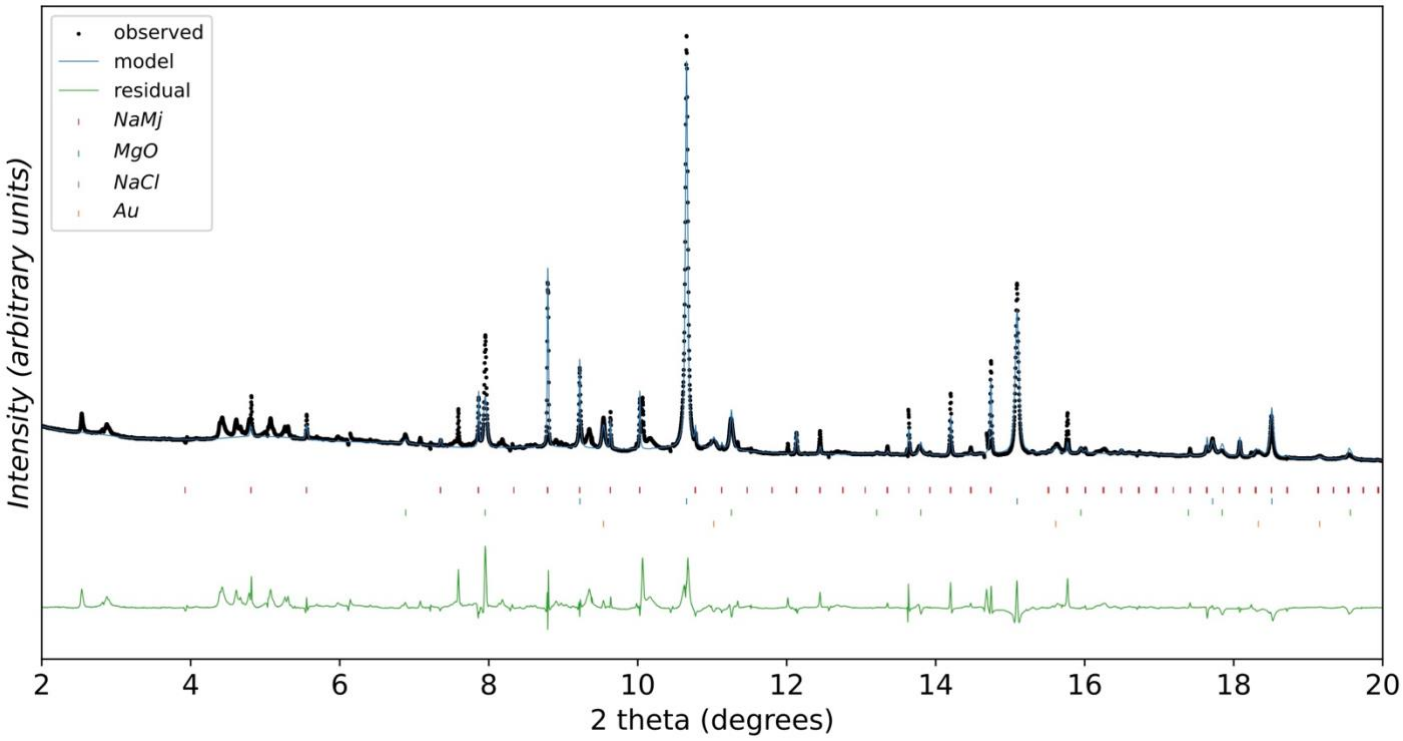

Figure 2*: refined diffraction pattern of NaMj sample after decompression to ambient conditions. The unfitted peaks (e.g. at ~ 2.5 and 7.5 degrees) are from small remnants of NaPx, which we did not wait to disappear due to the poor ultrasonic signal.*

To continue and complete our study we will request further beamtime. Based on the experience here we will additionally study samples of Mj_xPy_{1-x} solid solution, with x > 0.8. The reason for this decision is the the addition of small pyrope components expands the stability field of garnet to both lower pressure and temperature conditions (shrinking the fields of cpx and akimotoite stability that have to be transitted prior to data collection). Additionally, these compositions remain tetragonal at ambient conditions (Dymshits et al., 2013), unlike those with greater pyrope contents, thus still allowing the possible investigation of the cubic-tetragonal transitions. Additionally, we will only emply smaller 7/3 cells, which experience smaller pressure losses on initial heating, which will hopefully avoid back-transformation of starting materials.

References

Akaogi, M., & Akimoto, S. I. (1977). Pyroxene-garnet solid-solution equilibria in the systems $Mg_4Si_4O_{12}$-$Mg_3Al_2Si_3O_{12}$ and $Fe_4Si_4O_{12}$-$Fe_3Al_2Si_3O_{12}$ at high pressures and temperatures. *Physics of the Earth and Planetary Interiors*, *15*(1), 90-106.

Bindi, L., Dymshits, A. M., Bobrov, A. V., Litasov, K. D., Shatskiy, A. F., Ohtani, E., & Litvin, Y. A. (2011). Crystal chemistry of sodium in the Earth's interior: The structure of $Na_2MgSi_5O_{12}$ synthesized at 17.5 GPa and 1700 C. *American Mineralogist*, *96*(2-3), 447-450.

Dymshits, A. M., Bobrov, A. V., Bindi, L., Litvin, Y. A., Litasov, K. D., Shatskiy, A. F., & Ohtani, E. (2013). Na-bearing majoritic garnet in the $Na_2MgSi_5O_{12}$–$Mg_3Al_2Si_3O_{12}$ join at 11–20 GPa: Phase relations, structural peculiarities and solid solutions. *Geochimica et Cosmochimica Acta*, *105*, 1-13.

Dziewonski, A.M., and Anderson, D.L. (1981) Preliminary reference Earth model. Physics of the Earth and Planetary Interiors, 25, 297–356.

Hazen, R. M., Downs, R. T., Conrad, P. G., Finger, L. W., & Gasparik, T. (1994). Comparative compressibilities of majorite-type garnets. *Physics and Chemistry of Minerals*, *21*(5), 344-349.

Heinemann, S., Sharp, T. G., Seifert, F., & Rubie, D. C. (1997). The cubic-tetragonal phase transition in the system majorite ($Mg_4Si_4O_{12}$)–pyrope ($Mg_3Al_2Si_3O_{12}$), and garnet symmetry in the Earth's transition zone. *Physics and Chemistry of Minerals*, *24*(3), 206-221.

Holland, T. J., Hudson, N. F., Powell, R., & Harte, B. (2013). New thermodynamic models and calculated phase equilibria in NCFMAS for basic and ultrabasic compositions through the transition zone into the uppermost lower mantle. *Journal of Petrology*, *54*(9), 1901-1920.

Irifune, T., Higo, Y., Inoue, T., Kono, Y., Ohfuji, H., & Funakoshi, K. (2008). Sound velocities of majorite garnet and the composition of the mantle transition region. *Nature*, *451*(7180), 814-817.

Pacalo, R. E. G., & Weidner, D. J. (1997). Elasticity of majorite, $MgSiO_3$ tetragonal garnet. *Physics of the Earth and Planetary Interiors*, *99*(1-2), 145-154.

Ritsema, J., Deuss, A., van Heijst, H.J., and Woodhouse, J.H. (2011) S40RTS: a degree-40 shear-velocity model for the mantle from new Rayleigh wave dispersion, teleseismic traveltime and normal-mode splitting function measurements. Geophysical Journal International, 184, 1223–1236.